data

MDPI

Article

Regionalization of a Landscape-Based Hazard Index of Malaria Transmission: An Example of the State of Amapá, Brazil

Zhichao Li [1,2,*], Thibault Catry [2], Nadine Dessay [2], Helen da Costa Gurgel [3], Cláudio Aparecido de Almeida [4], Christovam Barcellos [5] and Emmanuel Roux [2,*]

1 Ministry of Education Key Laboratory for Earth System Modeling, Department of Earth System Science, Tsinghua University, Beijing 100084, China
2 ESPACE-DEV, UMR 228 IRD/UM/UR/UG, Institut de Recherche pour le Développement (IRD), 500 rue Jean-François Breton, Montpellier 34000, France; thibault.catry@ird.fr (T.C.); nadine.dessay@ird.fr (N.D.)
3 Department of Geography, University of Brasilia, 70910-900 Brasilia, Brazil; helengurgel@unb.br
4 National Institute for Space Research (INPE)—Image Processing Division, Av. dos Astronautas, 1758, 12227-010 São José dos Campos, Brazil; claudio.almeida@inpe.br
5 Institute of Scientific and Technological Communication and Information in Health (ICICT), Oswaldo Cruz Foundation (FIOCRUZ), Av. Brasil 4365, Manguinhos, 21045-900 Rio de Janeiro, Brazil; xris@fiocruz.br
* Correspondence: zhichaoli@mail.tsinghua.edu.cn (Z.L.); emmanuel.roux@ird.fr (E.R.); Tel.: +86-10-62786071 (Z.L.); +33-467-415125 (E.R.)

Received: 19 September 2017; Accepted: 1 November 2017; Published: 2 November 2017

Abstract: Identifying and assessing the relative effects of the numerous determinants of malaria transmission, at different spatial scales and resolutions, is of primary importance in defining control strategies and reaching the goal of the elimination of malaria. In this context, based on a knowledge-based model, a normalized landscape-based hazard index (*NLHI*) was established at a local scale, using a 10 m spatial resolution *forest vs. non-forest* map, landscape metrics and a spatial moving window. Such an index evaluates the contribution of landscape to the probability of human-malaria vector encounters, and thus to malaria transmission risk. Since the knowledge-based model is tailored to the entire Amazon region, such an index might be generalized at large scales for establishing a regional view of the landscape contribution to malaria transmission. Thus, this study uses an open large-scale land use and land cover dataset (i.e., the 30 m TerraClass maps) and proposes an automatic data-processing chain for implementing *NLHI* at large-scale. First, the impact of coarser spatial resolution (i.e., 30 m) on *NLHI* values was studied. Second, the data-processing chain was established using R language for customizing the spatial moving window and computing the landscape metrics and *NLHI* at large scale. This paper presents the results in the State of Amapá, Brazil. It offers the possibility of monitoring a significant determinant of malaria transmission at regional scale.

Keywords: malaria; landscape-based hazard index; large-scale; Amazon

1. Introduction

Malaria remains a major vector-borne disease in the world with an estimated 212 million new cases and an estimated 429,000 deaths in 2015, which mostly occur in tropical and sub-tropical regions [1]. In South America, the Amazonian region attracts the majority of malaria cases and exhibits a high transmission risk [1]. Although malaria is treatable and preventable [2], its elimination is difficult in Latin America, which requires vector control strategies to be adapted to local constraints, depending on a knowledge of the interaction between vector, human and environment [3]. The definition of new control strategies at different scales remains a challenge for researchers and policymakers who could benefit from the prior knowledge of malaria transmission risk at suitable scale [4]. Identifying malaria

risk factors and modeling malaria transmission processes in endemic and epidemic regions is highly valuable for a better understanding of malaria transmission [5,6].

Deforestation in the Amazon rainforest has been identified as a significant factor of malaria risk [7–9]. Stefani et al. [10] carried out a systematic review and formalized the elements of consensus regarding the relationship between malaria transmission by the main malaria vector in this region, *Anopheles darlingi*, and deforestation in a knowledge-based model: (i) deforested areas can supply favorable conditions for malaria vector breeding and feeding because they are usually accompanied by the presence of human populations and activities; and (ii) forested areas can provide resting sites for adult vectors that return to forest after their blood-meal in deforested areas. Based on this model, a normalized landscape-based hazard index (*NLHI*) was established for describing the contribution of landscape on malaria transmission. This index was defined as the linear normalization of the product of two landscape metrics: percentage of *forest* (*pF*) and density of *forest—non-forest* edges (*ED*), computed within a discoidal moving window with a radius of 400 m (see [11] for more details). This index was applied and validated in the cross-border area between French Guiana and Brazil (Figure 1), using a 10 m spatial resolution *forest vs. non-forest* land cover map derived from SPOT 5 multispectral imagery and obtained in [11].

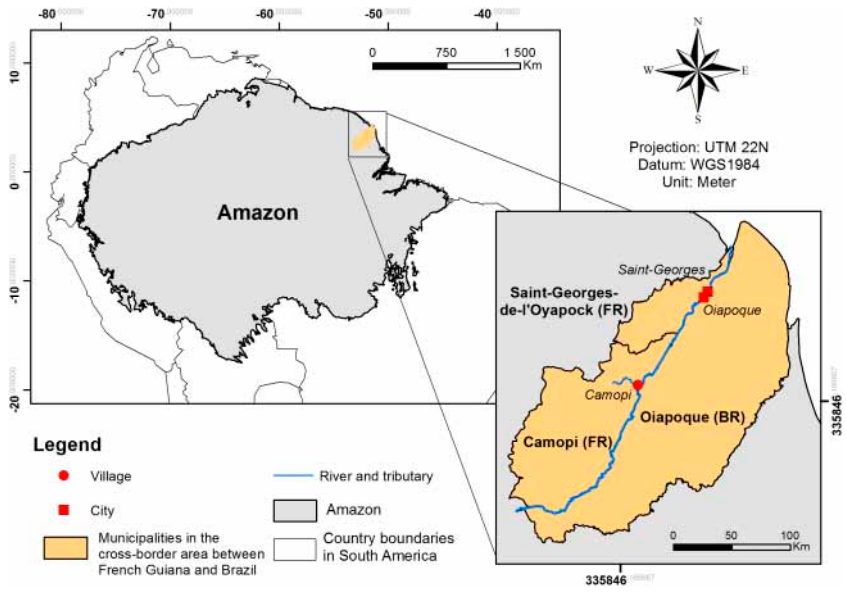

Figure 1. The entire Amazon region and the cross-border area between French Guiana and Brazil.

Because the knowledge-based model is tailored to the entire Amazonian region, *NLHI* established at a local spatial scale might be generalized at large scale within this region (Figure 1) to give a regional view of the landscape distribution on malaria transmission. The selection of appropriate input data (i.e., the large-scale *forest vs. non-forest* maps) needs consideration. In fact, accurately mapping land use and land cover (LULC) in large-scale tropical regions is a challenge due to the limitations of remote sensing data and complex biophysical environments [12]. First, low spatial resolution sensors, such as MODIS (250 m, 500 m and 1000 m), often provide repeated observations of the earth's surface from regional to global scale, but cannot detect certain spatial details of landscape features. However, *NLHI* computation should be realized in a discoidal moving window of 400 m. Low resolution imageries appear to be inadequate for estimating the edge between forest and non-forest patches. Second, high spatial resolution sensors, such as SPOT 5, can detect small scale landscape features [13], but LULC mapping with such images at regional scale is still particularly costly in respect of computing resources. Third, the frequent cloud cover in tropical regions often results in missing information in optical data [14–16].

Landsat data is a good choice for mostly overcoming all these obstacles and mapping large-scale LULC maps in tropical regions because of: (i) systematic data acquisition; (ii) global coverage; and (iii) high temporal repetitivity [17]. It has been extensively used for LULC mapping [18,19] or monitoring forest cover and its changes [20,21]. Particularly, the 30 m TerraClass LULC maps derived from Landsat data by the collaboration of Brazilian National Institute for Space Research (INPE) and Brazilian Agricultural Research Corporation (EMBRAPA) provided a detailed follow-up of deforested areas in the Brazilian Legal Amazonian region from 2004 (see [22] for more details). It was selected as a basis for producing the *forest vs. non-forest* map and then for implementing the large-scale *NLHI*.

Being built with landscape metrics, *NLHI* can be expected to be significantly affected by the changes in spatial resolution of input data and computation window size [23–26]. A fixed extent, corresponding to a discoidal moving window with a radius of 400 m, was used for the *NLHI* computation. Therefore, the effect of a coarser spatial resolution (i.e., 30 m) on the *NLHI* values was the only issue that needed to be investigated before implementing this index.

In this context, the objectives of this article are: (1) to evaluate the impact of the spatial resolution deterioration (i.e., from 10 m to 30 m) on the *NLHI* values; and (2) to develop and apply an automatic data-processing chain for computing the *NLHI* at large scale using the 30 m land cover map.

2. Materials and Methods

2.1. Assessing the Effect of a Coarser Spatial Resolution on NLHI Values

In order to assess the effects of spatial resolution on *NLHI* values, a 30 m *forest vs. non-forest* map was simulated by resampling the native one (i.e., the 10 m *forest vs. non-forest* map obtained in [11]) with a majority filter. The 30 m *NLHI* (denoted as $NLHI_{sim}$ hereafter) was then computed using the reduced-resolution map. Secondly, $NLHI_{sim}$ was compared with the native index (i.e., the 10 m *NLHI* obtained in [11]), which was resampled to a 30 m resolution (denoted as $NLHI_{val}$ hereafter) using a median filter, in order to define the reference values of the index.

A comparative study was performed on the values of $NLHI_{sim}$ and $NLHI_{val}$ and the capacity of the two indices to explain malaria incidence rates. $NLHI_{sim}$ was then compared with $NLHI_{val}$ using the values extracted from 1000 randomly selected points. A pair of reduced-resolution *NLHIs* (i.e., $NLHI_{sim}$ and $NLHI_{val}$) were statistically compared by computing a linear regression model.

Moreover, $NLHI_{sim}$ was also compared to *P. falciparum* incidence rates observed in the 28 hamlets comprising the village of Camopi in French Guiana (see more details of the epidemiological data in [11,27–29]. The Pearson (*r*) and Spearman (*rho*) correlation coefficients and the linear regression coefficient of determination (R^2) were calculated between $NLHI_{sim}$ and incidence rates by considering: (i) all the hamlets of Camopi; (ii) only the hamlets with non-null incidence rate values.

The overall methodology is summarized in Figure 2.

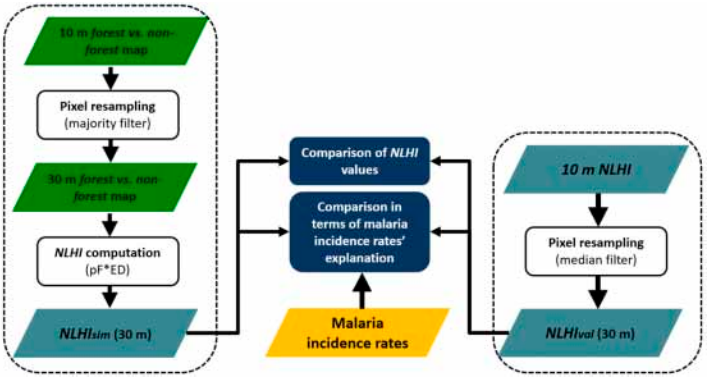

Figure 2. Flowchart of the evaluation of the impact of coarser spatial resolution on the normalized landscape-based hazard index (*NLHI*) values.

2.2. Large-Scale Implementation of NLHI

2.2.1. Input Data: TerraClass© product

The TerraClass LULC product covering the Brazilian Legal Amazon region (9 states of Brazil) is suitable for large-scale *NLHI* implementation. In fact, TerraClass is a project that was set up in 2009 by INPE in partnership with EMBRAPA in order to better understand the origin and consequences of the Brazilian Amazon deforestation. The nomenclature for TerraClass classification is presented in Figure 3. This dataset has been available since 2004 and has been updated every two years since 2008. For each date, the final product corresponds to a LULC map with a 30 m spatial resolution for each state in the Brazilian Legal Amazon. In this study, the TerraClass 2008 of the State of Amapá (Figure 3) was chosen for testing an automatic processing chain for the production of the large-scale *NLHI*.

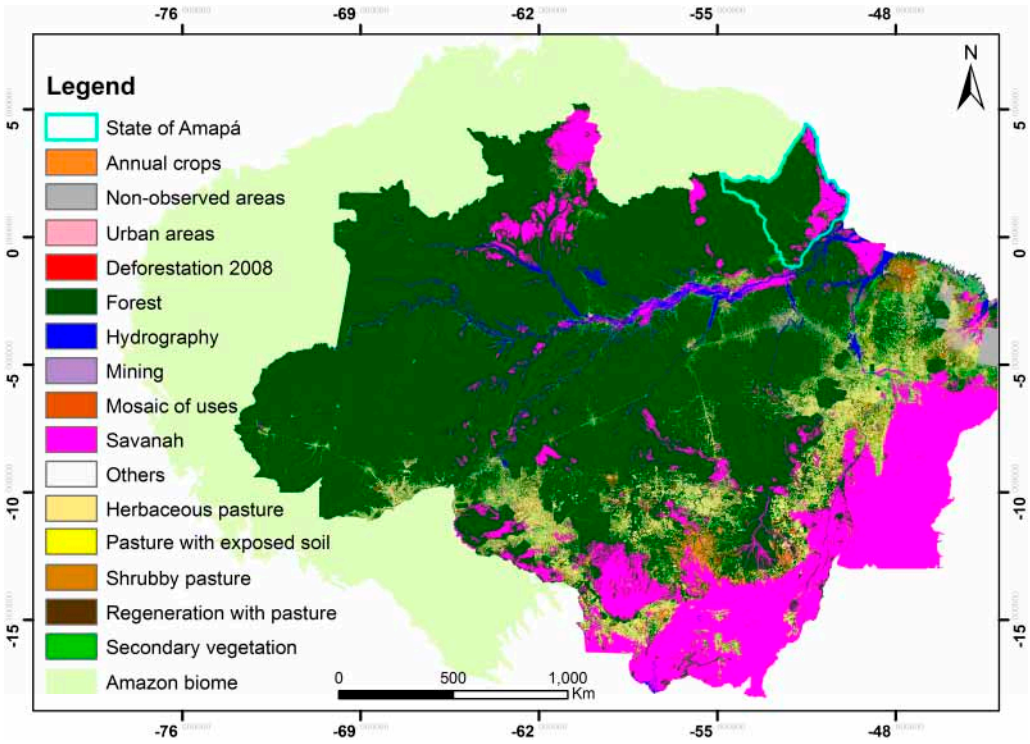

Figure 3. TerraClass 2008 map for the entire Brazilian Legal Amazon (source: Brazilian National Institute for Space Research (INPE)).

2.2.2. Large-Scale *NLHI* Implementation

Building the large-scale *NLHI* required the following steps: (1) the reclassification of input TerraClass map. In this study, the TerraClass of the State of Amapá was post-processed with the following procedures: (i) the class forest was denoted as ***forest*** hereafter, and the other classes were merged and denoted as ***non-forest*** hereafter; (ii) the non-observed areas, which are not possible to be interpreted by the Landsat data, were set to ***NoData*** and excluded from the *NLHI* computation, as the information of the Earth's surface is unclear in these areas; (2) the division of input data to allow parallel computation processing. The *forest vs. non-forest* map of the State of Amapá was divided into numerous overlapping blocks, which are the rectangular areas having the same sizes. Each block overlaps with the neighboring ones to take into account the border effect in the computation of landscape metrics hereafter (in step 4); (3) the selection of requisite blocks. Only the blocks including forest (value = *1*) and non-forest (value = *0*) were embedded in the following steps. In fact, the *NLHI* value is null in the blocks where either *forest* or *non-forest* class is absent, as no border between the two classes exists in this case; (4) the customization of a spatial moving window and the computation of

metrics (i.e., *pF* and *ED*) using the selected *forest vs. non-forest* blocks *via* moving window analysis. This window refers to a discoidal with a radius of 400 m, which was passed over each pixel of the selected blocks and returned the values of metrics back to the focal pixel. The returning values of metrics were set to *NoData*, while the window partly lay outside the input block or contained at least one *NoData* pixel (in our case, the border effect and *NoData* effect, respectively). Thus, the width of overlap had to be greater than or equal to the diameter of moving window (i.e., 400 × 2 m), so that the resulting blocks could be spliced together with the adjacent ones. A value of 960 m was subjectively chosen in this study; (5) the mosaic of the metric blocks for producing one large-scale map per metric (i.e., large-scale *pF* and *ED*); (6) the normalization of large-scale metrics. The normalization was executed for scaling the values of metrics between 0 and 1; (7) the computation of *NLHI*. The normalized large-scale *pF* and *ED* were combined using a product operator for producing the large-scale *NLHI*.

For reducing the computation time, multi-processors parallel computing was then applied in the third, fourth and fifth steps which took an enormous amount of time. All computations were implemented using R programming language. The overall methodology is summarized in Figure 4.

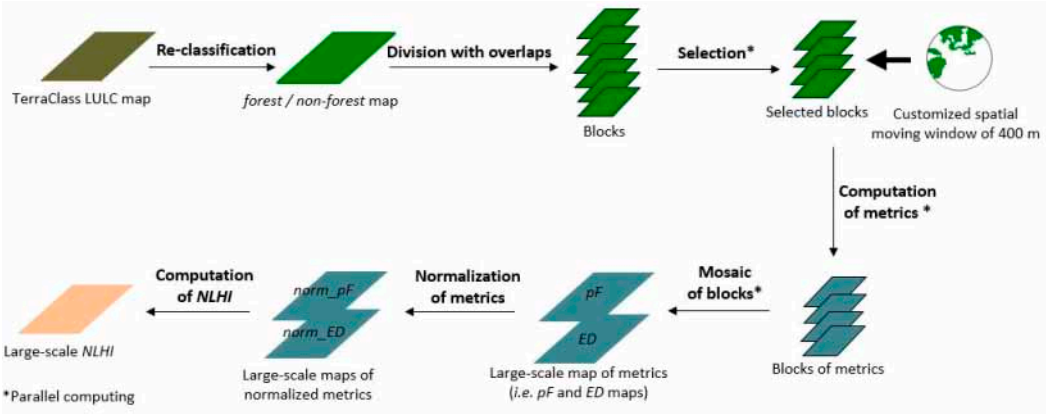

Figure 4. Summarized method of large-scale *NLHI* implementation.

3. Results

3.1. Within-Sensor Comparison between $NLHI_{sim}$ and $NLHI_{val}$

Figure 5 represents the linear regression between $NLHI_{sim}$ and $NLHI_{val}$. The coefficient of determination is 0.9886. This significant value shows that the *NLHI* was very little affected by the degradation of the spatial resolution of the *forest vs. non-forest* map from 10 to 30 m. In fact, the *NLHI* maintains a comparable capacity of discrimination. The prediction interval of $NLHI_{sim}$ as a function of $NLHI_{val}$ is 0.05. These results demonstrate the feasibility of implementing *NLHI* using 30 m spatial resolution LULC maps.

3.2. Relationship between NLHI Values and Malaria Incidence Rates

Figure 6 presents the *P. falciparum* incidence rates for the 28 hamlets of Camopi, as a function of the $NLHI_{sim}$ values. Table 1 shows the results of the correlation analysis between incidence rates and $NLHI_{sim}$, as well as the results obtained with 10 m resolution *NLHI* obtained in [11]. The results exhibit a very significant (p-values < 0.001) relationship between $NLHI_{sim}$ and the non-null incidence rates, with a Pearson correlation coefficient (r), a Spearman correlation coefficient (*rho*) and a coefficient of determination (R^2) equal to 0.80, 0.76 and 0.64, respectively. Results obtained with $NLHI_{sim}$ are very similar to those obtained with the native 10 m *NLHI* and even slightly superior.

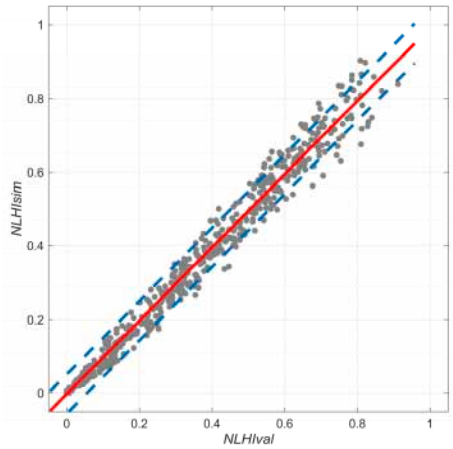

Figure 5. $NLHI_{sim}$ values as a function of $NLHI_{val}$. The line represents the regression line obtained using a linear regression model.

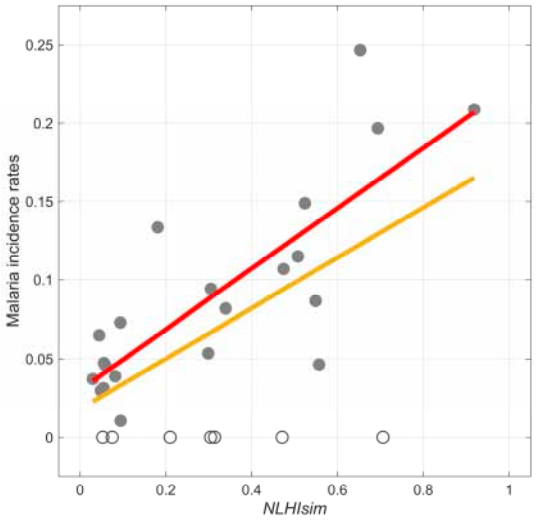

Figure 6. *P. falciparum* incidence rate values as a function of $NLHI_{sim}$. Dots and circle correspond to non-null and null incidence rates, respectively. Red and yellow lines represent the regression lines with non-null incidence rates and all the incidence rates, respectively, using a linear regression model.

Table 1. Results of the correlation analysis between *P. falciparum* incidence rates, $NLHI_{sim}$ and the native one. The values correspond to the Pearson correlation coefficient, *r*; the Spearman rank correlation coefficient, *rho*; and the coefficient of determination of a linear regression, R^2. Among these, the non-bold and bold values represent the results obtained with $NLHI_{sim}$ and the native *NLHI*, respectively. One or two asterisks correspond to a *p*-value lower than or equal to 0.01 and 0.001, respectively.

Correlation Analysis	*r*	*rho*	R^2
Whole dataset	0.60 **	0.44	0.36 **
	0.59 **	0.43	0.35 **
Non-null incidence rates only	0.80 **	0.76 **	0.64 **
	0.79 **	0.75 **	0.63 **

Notes: ** *p*-value $\leq$ 0.001.

3.3. Large-Scale NLHI

Figure 7 shows the *NLHI* in the State of Amapá (Figure 7b) resulting from the 30 m *forest vs. non-forest* map (Figure 7a), which was derived from the TerraClass LULC map of 2008. Figure 7c,d provide a more intuitive and detailed view of *NLHI* around Amapari city.

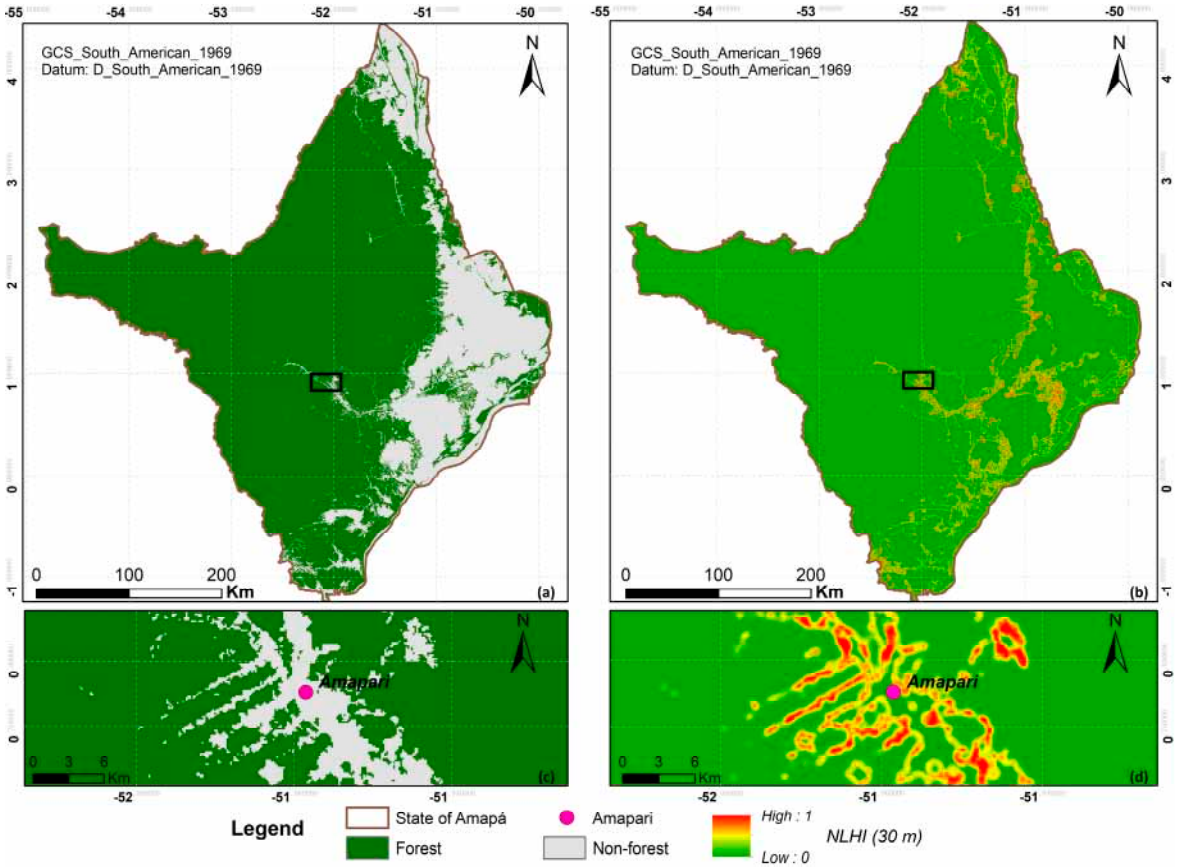

Figure 7. Results of large-scale *NLHI* computation. (**a**) *Forest vs. non-forest* map in the State of Amapá; (**b**) map of *NLHI* of the state; (**c**) Zoom of *forest vs. non-forest* map of Amapari; and (**d**) the corresponding *NLHI* map of Amapari.

4. Discussion

Changing spatial resolution from 10 m to 30 m does not significantly affect the performance and interpretation of *NLHI*. This simulation process permits us to assess the sensitivity of *NLHI* to spatial resolution only. In fact, any other changes in the input LULC raster have therefore been avoided, that is: (1) the changes related to sensor-specific characteristics such as systematic, radiometric and spectral features; (2) the scene-specific variations, notably changes in atmospheric conditions; (3) the differences due to the use of different satellite sensors [30]; and (4) the different classification methods. In addition, the result of the comparison between $NLHI_{sim}$ and actual incidence rates stated that the 30 m spatial resolution does not weaken the ability of the *NLHI* to reflect and quantify the contribution of the *forest vs. non-forest* landscapes to malaria transmission.

The LULC product derived from the TerraClass project was preferred as the input data for computing the *NLHI* because its objective is to map the different land use types in deforested areas related to anthropogenic activities. The class *forest* in TerraClass product can be used to map the resting sites of adult mosquitoes, and the *forest* and *non-forest* borders can be associated with the encounter probability of human being and adult vectors. The global accuracy of TerraClass 2008 is 76.6%, with

a Kappa index of 0.67 [22]. Using the TerraClass product allows for the production of qualified *NLHI* maps on a regular basis.

We could also regularly realize the large-scale *forest/non-forest* map using the Sentinel-2 imagery having a similar temporal observation with Landsat imagery. However, optical imagery presents certain important limits in an equatorial and tropical context due to the cloud cover. In contrast, synthetic aperture radar (SAR) sensors using low-frequency microwaves enable the easy differentiation of the forest and others LULC types with their cloud-penetrating capacity and day and night measurements [31–36]. For example, the Japan Aerospace Exploitation Agency (JAXA) realized the 25 m global *forest vs. non-forest* maps using PALSAR/PALSAR-2 images, which include three land cover types (i.e., *forest*, *non-forest* and *hydrography*) [35,36]. These databases can fill the gaps in time of TerraClass database.

Several factors account for the relatively long computation time, but some of these could be easily overcome in the future: (i) all computations were implemented using a personal computer with a 6-core 3.7 GHz processor and a 32 Go Random Access Memory (RAM) whereas the High-Performance Computing (HPC) could be used; (ii) two calls to the quite costly R function *PatchStat* were used to implement the computation of the edge density metric and such implementation, as well as other parts of the code, can certainly be optimized; (iii) the range of spatial resolution could be investigated in order to obtain an "optimal" value for implementing *NLHI*, which would allow for a reduction of the computation time while still capturing detailed landscape features.

In this study, only the State of Amapá was considered for testing the data-processing chain, as it represents a relatively high malaria risk in the Brazilian Legal Amazonian region. But, HPC appears necessary for computing the *NLHI* in the entire Brazilian Legal Amazon region on a temporal basis.

The resulting large-scale *NLHI* map (Figure 7b) at a 30 m spatial resolution is able to quantify the interaction degree between forest and non-forest areas (Figure 7a) in the State of Amapá. This interaction modulates the encounter chance between the main malaria vector (i.e., *Anopheles darling*) and humans frequenting the non-forested areas. It also allows study such interaction at a more local spatial scale (Figure 7c). Consequently, *NLHI* contributes to the assessment of exposure risk to the main malaria vector in the region. Deforestation is not only provoked by mass forest destruction (e.g., forest cleaning for pasture land) but also by diffuse forest disturbances (e.g., roads and selective logging sites), which represent a higher risk of malaria transmission [37]. In the future, this large-scale *NLHI* map might be used for investigating the contribution of each deforestation pattern type on malaria transmission.

5. Conclusions

An automatic data-processing chain was established for the practical production of a landscape-based hazard index (*NLHI*) of malaria transmission at large scales. This algorithm was tested in the State of Amapá in Brazil using the TerraClass LULC map with a spatial resolution of 30 m. Such large-scale *NLHI* can give a broader view of the human risk of exposure to adult malaria vectors in this region, which might be used for establishing large-scale prevention and control of malaria transmission. More generally, this algorithm can be used in various studies that require large-scale analysis of landscape features, using landscape metrics and a spatial moving window.

Acknowledgments: This study was supported by the China Scholarship Council, the OSE-Guyamapá project (FEDER-Guyane, PO-Amazonie call), the TéléPal project (CNES-TOSCA 2014 call) and the GAPAM-Sentinela project (Guyamazon call). This work was also supported by public funds received in the framework of GEOSUD, a project (ANR-10-EQPX-20) of the program "Investissements d'Avenir" managed by the French National Research Agency. The authors wish to thank the INPE for providing the TerraClass dataset. The authors would also like to thank the members of the Environment, Societies and Health Risks inter-disciplinary work-group (ESoR group) of the ESPACE-DEV Unit for the constructive discussions that enriched the paper.

Author Contributions: Z.L. participated in the research design, data collection, analysis and interpretation, and prepared the manuscript. T.C. reviewed the manuscript. N.D. reviewed the manuscript. H.G. reviewed the manuscript. C.A. reviewed the manuscript. C.B. reviewed the manuscript. E.R. participated in the research design,

data collection, analysis and interpretation, and reviewed the manuscript. All authors read and approved the final manuscript.

Conflicts of Interest: The authors declare no conflict of interest.

Abbreviations

The following abbreviations are used in this manuscript:

ED	Edge density
EMBRAPA	Brazilian Agricultural Research Corporation
HPC	High Performance Computing
INPE	Brazilian National Institutes for Space Research
JAXA	Japan Aerospace Exploitation Agency
LULC	Land use and land cover
NLHI	Normalization landscape-based hazard index
pF	Proportion of the forest
RAM	Random Access Memory
SAR	Synthetic aperture radar

References

1. WHO. *World Malaria Repport 2016*; WHO: Geneva, Swizerland, 2016.
2. Vitor-Silva, S.; Siqueira, A.M.; de Souza Sampaio, V.; Guinovart, C.; Reyes-Lecca, R.C.; de Melo, G.C.; Monteiro, W.M.; Del Portillo, H.A.; Alonso, P.; Bassat, Q.; et al. Declining malaria transmission in rural Amazon: Changing epidemiology and challenges to achieve elimination. *Malar. J.* **2016**, *15*, 266. [CrossRef] [PubMed]
3. Alimi, T.O.; Fuller, D.O.; Quinones, M.L.; Xue, R.D.; Herrera, S.V.; Arevalo-Herrera, M.; Ulrich, J.N.; Qualls, W.A.; Beier, J.C. Prospects and recommendations for risk mapping to improve strategies for effective malaria vector control interventions in latin America. *Malar. J.* **2015**, *14*, 519. [CrossRef] [PubMed]
4. Alegana, V.A.; Atkinson, P.M.; Lourenco, C.; Ruktanonchai, N.W.; Bosco, C.; Erbach-Schoenberg, E.Z.; Didier, B.; Pindolia, D.; Le Menach, A.; Katokele, S.; et al. Advances in mapping malaria for elimination: Fine resolution modelling of plasmodium falciparum incidence. *Sci. Rep.* **2016**, *6*, 29628. [CrossRef] [PubMed]
5. Ye, Y.; Hoshen, M.; Kyobutungi, C.; Louis, V.R.; Sauerborn, R. Local scale prediction of plasmodium falciparum malaria transmission in an endemic region using temperature and rainfall. *Glob. Health Action* **2009**, *2*. [CrossRef]
6. Musset, L.; Pelleau, S.; Girod, R.; Ardillon, V.; Carvalho, L.; Dusfour, I.; Gomes, M.S.M.; Djossou, F.; Legrand, E. Malaria on the Guiana shield: A review of the situation in French Guiana. *Mem. Inst. Oswaldo Cruz* **2014**, *109*, 525–533. [CrossRef] [PubMed]
7. Vittor, A.Y.; Gilman, R.H.; Tielsch, J.; Glass, G.; Shields, T.; Lozano, W.S.; Pinedo-Cancino, V.; Patz, J.A. The effect of deforestation on the human-biting rate of *Anopheles darlingi*, the primary vector of Falciparum malaria in the Peruvian Amazon. *Am. J. Trop. Med. Hyg.* **2006**, *74*, 3–11. [PubMed]
8. Vittor, A.Y.; Pan, W.; Gilman, R.H.; Tielsch, J.; Glass, G.; Shields, T.; Sanchez-Lozano, W.; Pinedo, V.V.; Salas-Cobos, E.; Flores, S.; et al. Linking deforestation to malaria in the Amazon: Characterization of the breeding habitat of the principal malaria vector, *Anopheles darlingi*. *Am. J. Trop. Med. Hyg.* **2009**, *81*, 5–12. [PubMed]
9. Barros, F.S.; Honorio, N.A. Deforestation and malaria on the Amazon frontier: Larval clustering of *Anopheles darlingi* (Diptera: Culicidae) determines focal distribution of malaria. *Am. J. Trop. Med. Hyg.* **2015**, *93*, 939–953. [CrossRef] [PubMed]
10. Stefani, A.; Dusfour, I.; Cruz, M.C.B.; Dessay, N.; Galardo, A.K.R.; Galardo, C.D.; Girod, R.; Gomes, M.S.M.; Gurgel, H.; Lima, A.C.F.; et al. Land cover, land use and malaria in the amazon: A systematic literature review of studies using remotely sensed data. *Malar. J.* **2013**, *12*. [CrossRef] [PubMed]
11. Li, Z.; Roux, E.; Dessay, N.; Girod, R.; Stefani, A.; Nacher, M.; Moiret, A.; Seyler, F. Mapping a knowledge-based malaria hazard index related to landscape using remote sensing: Application to the cross-border area between French Guiana and Brazil. *Remote Sens.* **2016**, *8*, 319. [CrossRef]

12. Lu, D.; Batistella, M.; Li, G.; Moran, E.; Hetrick, S.; Freitas, C.D.; Dutra, L.V.; Sant'anna, S.J. Land use/cover classification in the Brazilian Amazon using satellite images. *Pesq. agropec. bras.* **2012**, *47*. [CrossRef] [PubMed]
13. Wang, G.; Liu, J.; He, G. A method of spatial mapping and reclassification for high-spatial-resolution remote sensing image classification. *Sci. World J.* **2013**, *2013*, 192982. [CrossRef] [PubMed]
14. Asner, G.P. Cloud cover in Landsat observations of the Brazilian Amazon. *Int. J. Remote Sens.* **2001**, *22*, 3855–3862. [CrossRef]
15. Souza, J.C.; Siqueira, J.; Sales, M.; Fonseca, A.; Ribeiro, J.; Numata, I.; Cochrane, M.; Barber, C.; Roberts, D.; Barlow, J. Ten-year Landsat classification of deforestation and forest degradation in the Brazilian Amazon. *Remote Sens.* **2013**, *5*, 5493–5513. [CrossRef]
16. Tiner, R.W.; Lang, M.W.; Klemas, V.V. *Remote Sensing of Wetlands: Applications and Advances*; CRC Press: Boca Raton, FL, USA, 2015.
17. Powell, S.L.; Pflugmacher, D.; Kirschbaum, A.A.; Kim, Y.; Cohen, W. Moderate resolution remote sensing alternatives: A review of Landsat-like sensors and their applications. *J. Appl. Remote Sens.* **2007**, *1*, 012506.
18. Gong, P.; Wang, J.; Yu, L.; Zhao, Y.; Zhao, Y.; Liang, L.; Niu, Z.; Huang, X.; Fu, H.; Liu, S.; et al. Finer resolution observation and monitoring of global land cover: First mapping results with Landsat TM and ETM+ data. *Int. J. Remote Sens.* **2013**, *34*, 2607–2654. [CrossRef]
19. Baraldi, A.; Puzzolo, V.; Blonda, P.; Bruzzone, L.; Tarantino, C. Automatic spectral rule-based preliminary mapping of calibrated Landsat tm and etm+ images. *IEEE Trans. Geosci. Remote Sens.* **2006**, *44*, 2563–2586. [CrossRef]
20. Kim, D.H.; Sexton, J.O.; Noojipady, P.; Huang, C.Q.; Anand, A.; Channan, S.; Feng, M.; Townshend, J.R. Global, Landsat-based forest-cover change from 1990 to 2000. *Remote Sens. Environ.* **2014**, *155*, 178–193. [CrossRef]
21. Song, D.-X.; Huang, C.; Sexton, J.O.; Channan, S.; Feng, M.; Townshend, J.R. Use of Landsat and corona data for mapping forest cover change from the mid-1960s to 2000s: Case studies from the eastern united states and central brazil. *ISPRS* **2015**, *103*, 81–92. [CrossRef]
22. Almeida, C.A.D.; Coutinho, A.C.; Esquerdo, J.C.D.M.; Adami, M.; Venturieri, A.; Diniz, C.G.; Dessay, N.; Durieux, L.; Gomes, A.R. High spatial resolution land use and land cover mapping of the brazilian legal amazon in 2008 using Landsat-5/TM and modis data. *Acta Amazon.* **2016**, *46*, 291–302. [CrossRef]
23. Hargis, C.D.; Bissonette, J.A.; David, J.L. The behavior of landscape metrics commonly used in the study of habitat fragmentation. *Landsc. Ecol.* **1998**, *13*, 167–186. [CrossRef]
24. Saura, S. Effects of minimum mapping unit on land cover data spatial configuration and composition. *Int. J. Remote Sens.* **2002**, *23*, 4853–4880. [CrossRef]
25. Frohn, R.; Hao, Y. Landscape metric performance in analyzing two decades of deforestation in the Amazon basin of rondonia, Brazil. *Remote Sens. Environ.* **2006**, *100*, 237–251. [CrossRef]
26. McGarigal, K.; Cushman, S.; Ene, E. *Fragstats v4: Spatial Pattern Analysis Program for Categorical and Continuous Maps*; University of Massachusetts, Amherst: Amherst, MA, USA; Available online: https://www.umass.edu/landeco/research/fragstats/fragstats.html (accessed on 1 April 2017).
27. Hustache, S.; Nacher, M.; Djossou, F.; Carme, B. Malaria risk factors in amerindian children in French Guiana. *Am. J. Trop. Med. Hyg.* **2007**, *76*, 619–625. [PubMed]
28. Stefani, A.; Hanf, M.; Nacher, M.; Girod, R.; Carme, B. Environmental, entomological, socioeconomic and behavioural risk factors for malaria attacks in amerindian children of Camopi, French Guiana. *Malar. J.* **2011**, *10*. [CrossRef] [PubMed]
29. Stefani, A.; Roux, E.; Fotsing, J.M.; Carme, B. Studying relationships between environment and malaria incidence in Camopi (French Guiana) through the objective selection of buffer-based landscape characterisations. *Int. J. Health Geogr.* **2011**, *10*. [CrossRef] [PubMed]
30. Theau, J.; Sankey, T.T.; Weber, K.T. Multi-sensor analyses of vegetation indices in a semi-arid environment. *Gisci. Remote Sens.* **2010**, *47*, 260–275. [CrossRef]
31. Thiel, C.; Drezet, P.; Weise, C.; Quegan, S.; Schmullius, C. Radar remote sensing for the delineation of forest cover maps and the detection of deforestation. *Forestry* **2006**, *79*, 589–597. [CrossRef]
32. Rahman, M.M.; Sumantyo, J.T.S. Mapping tropical forest cover and deforestation using synthetic aperture radar (SAR) images. *Appl. Geomat.* **2010**, *2*, 113–121. [CrossRef]

33. Kellndorfer, J.; Cartus, O.; Bishop, J.; Walker, W.; Holecz, F. Large scale mapping of forests and land cover with synthetic aperture radar data. In *Land Applications of Radar Remote Sensing*; Holecz, F., Pasquali, P., Milisavljevic, N., Closson, D., Eds.; InTech: London, UK, 2014.
34. Shimada, M.; Itoh, T.; Motooka, T.; Watanabe, M.; Shiraishi, T.; Thapa, R.; Lucas, R. New global forest/non-forest maps from ALOS PALSAR data (2007–2010). *Remote Sens. Environ.* **2014**, *155*, 13–31. [CrossRef]
35. Shimada, M.; Itoh, T.; Motooka, T.; Watanabe, M.; Thapa, R. High-resolution satellite radar for mapping changes in global forest cover. *SPIE Sens. Meas.* **2015**. [CrossRef]
36. Ningthoujam, R.; Tansey, K.; Balzter, H.; Morrison, K.; Johnson, S.; Gerard, F.; George, C.; Burbidge, G.; Doody, S.; Veck, N.; et al. Mapping forest cover and forest cover change with airborne s-band radar. *Remote Sens.* **2016**, *8*, 577. [CrossRef]
37. Hahn, M.B.; Gangnon, R.E.; Barcellos, C.; Asner, G.P.; Patz, J.A. Influence of deforestation, logging, and fire on malaria in the Brazilian Amazon. *PLoS ONE* **2014**, *9*, e85725. [CrossRef] [PubMed]

© 2017 by the authors. Licensee MDPI, Basel, Switzerland. This article is an open access article distributed under the terms and conditions of the Creative Commons Attribution (CC BY) license (http://creativecommons.org/licenses/by/4.0/).